NeuroImage: Clinical 27 (2020) 102315

Contents lists available at ScienceDirect

NeuroImage: Clinical

journal homepage: www.elsevier.com/locate/ynicl

Structural MRI outcomes and predictors of disease progression in amyotrophic lateral sclerosis

Edoardo G. Spinelli[a,c,g], Nilo Riva[b], Paola M.V. Rancoita[e], Paride Schito[c], Alberto Doretti[f], Barbara Poletti[f], Clelia Di Serio[e], Vincenzo Silani[f,h], Massimo Filippi[a,c,d,g], Federica Agosta[a,g,*]

[a] Neuroimaging Research Unit, Institute of Experimental Neurology, Division of Neuroscience, IRCCS San Raffaele Scientific Institute, Milan, Italy
[b] Neurorehabilitation Unit, IRCCS San Raffaele Scientific Institute, Milan, Italy
[c] Neurology Unit, IRCCS San Raffaele Scientific Institute, Milan, Italy
[d] Neurophysiology Unit, IRCCS San Raffaele Scientific Institute, Milan, Italy
[e] University Centre for Statistics in the Biomedical Sciences (CUSSB), Vita-Salute San Raffaele University, Milan, Italy
[f] Department of Neurology and Laboratory of Neuroscience, IRCCS Istituto Auxologico Italiano, Milan, Italy
[g] Vita-Salute San Raffaele University, Milan, Italy
[h] "Dino Ferrari" Center, Department of Pathophysiology and Transplantation, Università degli Studi di Milano, Milan, Italy

ARTICLE INFO

Keywords:
Amyotrophic lateral sclerosis
Structural MRI
Prognosis
Cortical thickness
Diffusion tensor MRI

ABSTRACT

Background and aims: Considering the great heterogeneity of amyotrophic lateral sclerosis (ALS), the identification of accurate prognostic predictors is fundamental for both the clinical practice and the design of treatment trials. This study aimed to explore the progression of clinical and structural brain changes in patients with ALS, and to assess magnetic resonance imaging (MRI) measures of brain damage as predictors of subsequent functional decline.

Methods: 50 ALS patients underwent clinical evaluations and 3 T MRI scans at regular intervals for a maximum of 2 years (total MRI scans = 164). MRI measures of cortical thickness, as well as diffusion tensor (DT) metrics of microstructural damage along white matter (WM) tracts were obtained. Voxel-wise regression models and longitudinal mixed-effects models were used to test the relationship between clinical decline and baseline and longitudinal MRI features.

Results: The rate of decline of the ALS Functional Rating Scale revised (ALSFRS-r) was significantly associated with the rate of fractional anisotropy (FA) decrease in the body of the corpus callosum (CC). Corticospinal tract (CST) and CC-body alterations had a faster progression in patients with higher baseline ALSFRS-r scores and greater CC-body disruption at baseline. Lower FA of the cerebral peduncle was associated with faster subsequent clinical progression.

Conclusions: In this longitudinal study, we identified a significant association between measures of WM damage of the motor tracts and functional decline in ALS patients. Our data suggest that a multiparametric approach including DT MRI measures of brain damage would provide an optimal method for an accurate stratification of ALS patients into prognostic classes.

1. Introduction

Amyotrophic lateral sclerosis (ALS) is a rapidly progressive, fatal neurodegenerative condition causing prominent motor impairment (Calvo et al., 2017). Considering the great heterogeneity of ALS clinical course, the identification of accurate biomarkers of progression and prognostic predictors is important for both the clinical practice and the design of treatment trials (Kiernan et al., 2011). Advanced magnetic resonance imaging (MRI) has recently emerged as a promising candidate to allow an objective assessment of central nervous system (CNS) damage in ALS patients *in vivo*, showing the progressive involvement of both motor and extra-motor networks (Agosta et al., 2018). However, relatively few longitudinal MRI studies have been published (Agosta et al., 2009; Bede and Hardiman, 2018; de Albuquerque et al., 2017; Kassubek et al., 2018; Keil et al., 2012; Kwan et al., 2012; Menke et al., 2018; van der Graaff et al., 2011), mirroring the difficulties in enrolling

* Corresponding author at: Neuroimaging Research Unit, Institute of Experimental Neurology, Division of Neuroscience, IRCCS San Raffaele Scientific Institute and Vita-Salute San Raffaele University, Via Olgettina, 60, 20132 Milan, Italy.
E-mail address: agosta.federica@hsr.it (F. Agosta).

https://doi.org/10.1016/j.nicl.2020.102315
Received 21 March 2020; Received in revised form 10 June 2020; Accepted 11 June 2020
Available online 17 June 2020

enough patients who could undergo an appropriate number of follow-up scans. Moreover, only few of these studies included a multi-parametric approach (Bede and Hardiman, 2018; de Albuquerque et al., 2017; Menke et al., 2018), and results regarding the pattern and the respective degree of grey matter (GM) and white matter (WM) degeneration over time are inconsistent. Finally, the relationship between structural alterations and the co-occurrent and subsequent evolution of functional impairment is far from being clarified (Menke et al., 2017).

The aim of the present study was to determine which measures of GM cortical thickness and WM diffusivity provided by structural and diffusion tensor (DT) MRI were most sensitive to the progression of neurodegeneration and clinical impairment in a cohort of non-demented ALS patients who were enrolled soon after their diagnosis and followed-up at a regular interval for up to 2 years. We also assessed the potential use of these metrics as predictors of subsequent functional decline.

2. Methods

2.1. Participants and study design

Fifty patients with sporadic possible (n = 10), probable laboratory-supported (n = 22), probable (n = 9) or definite (n = 9) ALS according to El Escorial revised criteria (Brooks et al., 2000) were prospectively recruited at two tertiary referral ALS clinics in Milan between October 2009 and October 2015 within the framework of a longitudinal project, including only individuals within the first year after clinical diagnosis (Table 1). Patients received a comprehensive evaluation including clinical and MRI assessments at study entry and every 3 months for the first year; clinical evaluations were also performed every 6 months for the subsequent year. All patients underwent at least two MRI scans at the scheduled timepoints (Fig. 1, average number of scans = 3.28 ± 1.55). A significant proportion developed respiratory problems that did not allow the acquisition of further MRI data, and several patients could not undergo clinical follow-up visits, due to severe motor disability. In these latter cases, the development of clinical milestones of progression was assessed by phone interview to caregivers. At baseline, a screening cognitive assessment including Mini Mental State Examination (Folstein et al., 1975) and fluency tests (Novelli et al., 1986) was obtained from all patients, who were non-demented according to frontotemporal dementia criteria (Rascovsky et al., 2011) at any timepoint. When necessary, Rascovsky criteria (Rascovsky et al., 2011) were applied retrospectively, based on patients' charts. The main demographic, clinical and cognitive features of included ALS patients are shown in Table 1. Forty-seven age- and sex-matched healthy controls were recruited by word of mouth, based on the following criteria: normal neurological assessment; MMSE score ≥ 28; no family history of neurodegenerative diseases. Healthy controls performed clinical, cognitive and MRI assessments at baseline. Exclusion criteria for all subjects were: medical illnesses or substance abuse that could interfere with cognitive functioning; any (other) major systemic, psychiatric, or neurological diseases; other causes of brain damage, including lacunae and extensive cerebrovascular disorders at MRI.

The study was approved by the institutional ethics committees of the IRCCS San Raffaele Scientific Institute and IRCCS Istituto Auxologico Italiano in Milan and all participants (or their caregivers) provided written informed consent prior to study inclusion.

2.2. Clinical evaluation

At study entry and each follow-up visit, an experienced neurologist blinded to MRI results performed clinical assessments, recording site of disease onset and disease duration at presentation. Disease severity was assessed using the ALS Functional Rating Scale-revised (ALSFRS-r) (Cedarbaum et al., 1999). The baseline rate of disease progression was defined according to the following formula: (48–ALSFRS-r score)/time between symptom onset and first visit. Muscular strength was assessed by manual muscle testing based on the Medical Research Council (MRC) scale, and clinical upper motor neuron (UMN) involvement was graded by totaling the number of pathological UMN signs on examination (Turner et al., 2004). Events of mortality (i.e., death or tracheostomy) were recorded either at the moment of clinical evaluations or by phone interview to caregivers until March 30, 2019.

2.3. MRI acquisition

Baseline and follow-up brain MRI scans were acquired on the same 3 T Philips Medical System Intera machine. The following brain MRI

Table 1
Demographic, clinical and cognitive characteristics at study entry in ALS patients and healthy controls (HC).

	ALS (n = 50)	HC (n = 47)	p
Sex, males (%)	35 (70%)	28 (60%)	0.30
Age at baseline (years)	59.8 ± 11.5	60.8 ± 8.1	0.66
Disease duration at baseline (months)	16.2 ± 10.3	–	–
ALSFRS-r at baseline [0–48]	41.5 ± 5.1	–	–
ALSFRS-r progression rate (decrease/month)	0.5 ± 0.4	–	–
Site of symptom onset (limb/bulbar)	40/10	–	–
El Escorial diagnosis at baseline (possible/probable lab-supported/probable/definite)	10/22/9/9	–	–
El Escorial diagnosis at last visit (possible/probable lab-supported/probable/definite)	0/4/28/18	–	–
Total MRC sum score [0–120]	108.0 ± 11.2	–	–
UMN score [0–16]	9.2 ± 4.6	–	–
MMSE (% of correct/administrable items)	96.7 ± 3.2	–	–
Phonemic fluency [normal range > 17] (Novelli et al., 1986)	29.7 ± 9.4	–	–
Index PF	6.5 ± 2.9		
Semantic fluency [normal range > 25] (Novelli et al., 1986)	39.2 ± 9.2	–	–
Index SF	5.2 ± 3.6		
Deceased or tracheotomized at censoring (%)	41 (82%)	–	–
Survival from onset (months)	46.2 ± 18.1	–	–
Survival from baseline visit (months)	30.6 ± 15.8	–	–

Values are reported as mean ± standard deviation or absolute and percentage frequency (%) for continuous and categorical variables, respectively. Differences between ALS patients and healthy controls were assessed using Mann-Whitney (for age), or Fisher test (for sex).
Abbreviations: ALS = amyotrophic lateral sclerosis; ALSFRS-r = ALS functional rating scale, revised version; HC = healthy controls; MMSE = Mini Mental State Examination; MRC = Medical Research Council scale for muscular strength; PF = phonemic fluency; SF = semantic fluency; UMN = upper motor neuron.

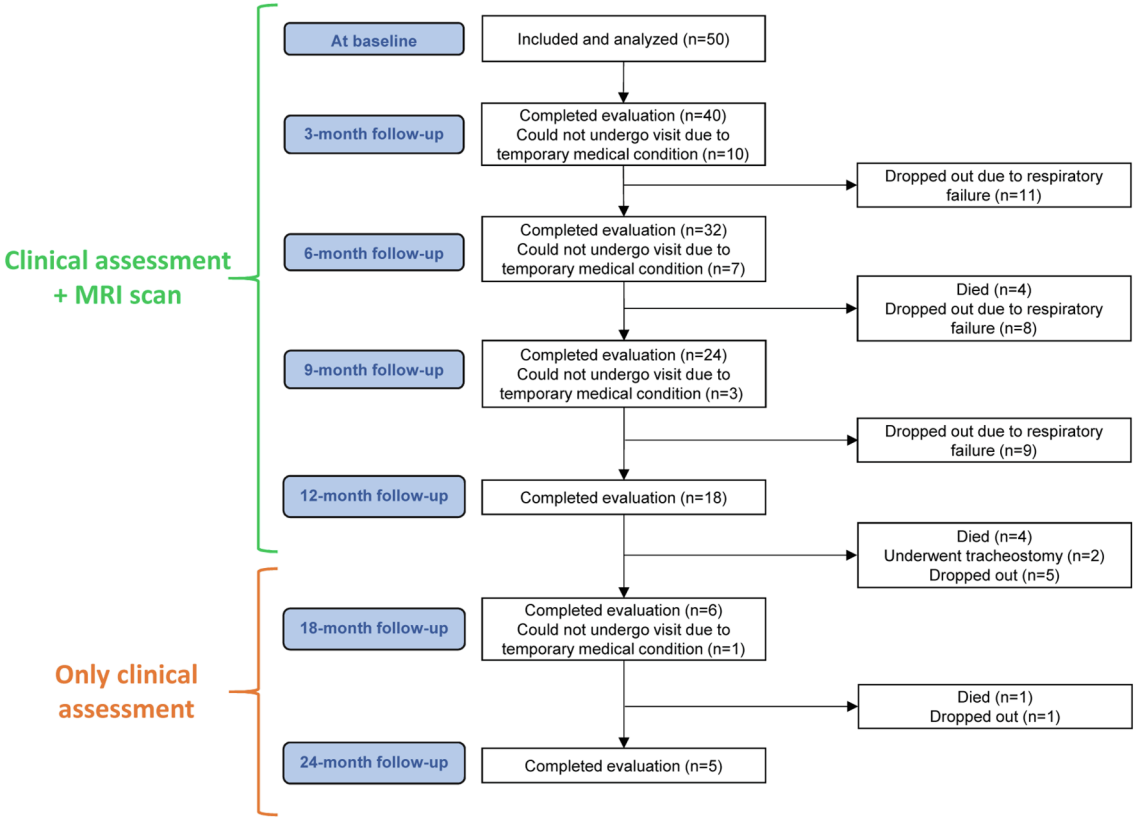

Fig. 1. Flow-chart describing design of the study and follow-up of ALS patients.

sequences were obtained from all subjects: T2-weighted spin echo (SE) (repetition time [TR] = 3500 ms; echo time [TE] = 85 ms; echo train length = 15; flip angle = 90°; 22 contiguous, 5-mm-thick, axial slices; matrix size = 512 × 512; field of view [FOV] = 230 × 184 mm^2); fluid-attenuated inversion recovery (TR = 11 s; TE = 120 ms; flip angle = 90°; 22 contiguous, 5-mm-thick, axial slices; matrix size = 512 × 512; FOV = 230 mm^2); 3D T1-weighted fast field echo (FFE) (TR = 25 ms, TE = 4.6 ms, flip angle = 30°, 220 contiguous axial slices with voxel size = 0.89 × 0.89 × 0.8 mm, matrix size = 256 × 256, FOV = 230 × 182 mm^2); and pulsed-gradient SE echo planar with sensitivity encoding (acceleration factor = 2.5, TR = 8986 ms, TE = 80 ms, 55 contiguous, 2.5 mm-thick axial slices, number of acquisitions = 2; acquisition matrix 96 × 96, with an in-plane pixel size of 1.89 × 1.89 mm and a FOV = 240 mm^2) diffusion gradients applied in 32 non-collinear directions using a gradient scheme which is standard on this system (gradient over-plus) and optimized to reduce echo time as much as possible. The b factor used was 1000 s/mm^2. Fat saturation was performed to avoid chemical shift artifacts. All slices were positioned to run parallel to a line that joins the most inferoanterior and inferoposterior parts of the corpus callosum.

2.4. MRI analysis

2.4.1. Cortical thickness measurement

Cortical reconstruction and estimation of cortical thickness were performed on the 3D T1-weighted images using the FreeSurfer image analysis suite, version 5.3 (http://surfer.nmr.mgh.harvard.edu/) (Fischl and Dale, 2000). After registration to Talairach space and intensity normalization, the process involved an automatic skull stripping, which removes extra-cerebral structures, cerebellum and brainstem, by using a hybrid method combining watershed algorithms and deformable surface models. Images were carefully checked for skull stripping errors. Then, images were segmented into GM, WM, and cerebrospinal fluid (CSF), cerebral hemispheres were separated, and subcortical structures divided from cortical components. The WM/GM boundary was tessellated and the surface was deformed following intensity gradients to optimally place WM/GM and GM/CSF borders, thus obtaining the WM and pial surfaces (Dale et al., 1999). Afterwards, surface inflation and registration to a spherical atlas were performed (Dale et al., 1999). Finally, cortical thickness was estimated as the average shortest distance between the WM boundary and the pial surface.

To evaluate longitudinal cortical changes in ALS patients, the serial 3D T1-weighted images of each subject were processed with the Freesurfer longitudinal stream (Reuter et al., 2012). Specifically, an unbiased within-subject template space and image was created from the available scans using a robust, inverse consistent registration. Several processing steps (including skull stripping, Talairach transforms, atlas registration, as well as spherical surface maps) were then initialized on the available scans, with common information from the within-subject template. This allowed to create surface maps of all the available timepoints (Reuter et al., 2012). Individual surface maps were registered to a common average surface and then smoothed using a Gaussian kernel of 10 mm full width half-maximum.

2.4.2. Diffusion tensor (DT) MRI analysis

DT MRI analysis was performed using the FMRIB software library (FSL) tools (http://www.fmrib.ox.ac.uk/fsl/fdt/index.html) and the JIM software (Xinapse Systems, Northants, UK, http://www.xinapse.com), as previously described (Agosta et al., 2013, 2014). The diffusion-weighted data underwent a careful quality check for head motion and were subsequently skull-stripped using the Brain Extraction Tool implemented in FSL. Using FMRIB's Linear Image Registration Tool (FLIRT), the two diffusion-weighted scans were coregistered by applying the rigid transformation needed to correct for position between the two b0 images (T2-weighted, but not diffusion-weighted). The rotation component was also applied to diffusion-weighted directions.

Eddy currents correction was performed using the JIM software (Horsfield, 1999). The DT was estimated on a voxel-by-voxel basis using DTIfit provided by the FMRIB Diffusion Toolbox. Maps of fractional anisotropy (FA), mean diffusivity (MD), axial diffusivity (axD) and radial diffusivity (radD) were obtained.

First, a whole-brain DT MRI analysis was performed using tract-based spatial statistics (TBSS) version 1.2 (http://www.fmrib.ox.ac.uk/fsl/tbss/index.html). FA volumes of all timepoints acquired from all subjects were aligned to a target image using the following procedure: (i) the FA template in standard space (provided by FSL) was selected as the target image, (ii) the nonlinear transformation that mapped each subject's FA to the target image was computed using the FMRIB's Nonlinear Image Registration Tool, and (iii) the same transformation was used to align each subject's FA to the standard space. A mean FA image was then created by averaging the aligned individual FA images and thinned to create a FA skeleton representing WM tracts common to all subjects. The FA skeleton was thresholded at a value of 0.2 to exclude voxels with low FA values, which are likely to include GM or CSF. Individual FA, MD, axD and radD data were projected onto this common skeleton. For the longitudinal analysis, skeletonised maps of each DT-derived metric of all available timepoints obtained from each ALS patient were fitted to a linear model using the Fitter tool in JIM7 (Horsfield, 1999) (www.xinapse.com): the model included a constant value, and time from baseline was set as independent variable; the obtained slope was retained for the statistical analysis.

Subsequently, based on the results of the whole-brain analysis, a region-of-interest (ROI) analysis was performed to assess the degeneration of motor WM tracts in greater detail. Masks of the body of the corpus callosum (CC-body) and four sub-regions of the corticospinal tract (CST) – i.e., the bulbo-pontine CST, cerebral peduncle, posterior limb of the internal capsule, and superior corona radiata – were obtained from the Johns Hopkins University (JHU) white-matter tractography atlas (Hua et al., 2008) and transformed onto the aligned, skeletonized TBSS data, in order to extract mean DT MRI metrics for each selected ROI at all timepoints. For CST data, the mean values of corresponding ROIs of the two hemispheres were averaged to obtain a single value.

2.5. Statistical analysis

2.5.1. Baseline MRI data

A cross-sectional vertex-by-vertex analysis using FreeSurfer, version 5.3 (http://surfer.nmr.mgh.harvard.edu/), was performed to assess differences of cortical thickness between ALS patients and healthy controls at baseline, adjusting for age and sex. The t-statistic was thresholded at $p < 0.05$, FDR-corrected for multiple comparisons.

DT MRI voxel-wise statistics were performed to compare FA, MD, axD and radD data between ALS patients and controls using a permutation-based inference tool for nonparametric statistical thresholding ("randomize", permutations = 5000) in FSL (https://fsl.fmrib.ox.ac.uk/fsl/fslwiki/Randomise/), adjusting for age and sex. Statistical maps were thresholded at $p < 0.05$, family-wise error (FWE) corrected for multiple comparisons at the cluster level using the threshold-free cluster enhancement option.

DT MRI parameters of the selected WM ROIs at baseline were compared between ALS patients and healthy controls using a Multivariate Analysis of Covariance (MANCOVA) test followed by post-hoc pairwise comparisons, adjusting for sex and age and applying Bonferroni correction for multiple comparisons. SPSS Statistics 22.0 was used.

2.5.2. Longitudinal MRI data

Longitudinal changes of cortical thickness occurring in ALS patients were assessed using Linear Mixed Effects Models in FreeSurfer v5.3 (Bernal-Rusiel et al., 2013) adjusting for age, sex, and ALSFRS-r score at baseline as fixed-effects covariates (without variable selection). Random effects were defined on the intercept. The t-statistic was thresholded at $p < 0.05$, FDR-corrected.

One-sample t-tests using the "randomize" voxel-wise statistical tool in FSL (permutations = 5000) were performed to assess the evolution of FA, MD, axD and radD slopes, adjusting for age, sex and baseline ALSFRS-r score. Statistical maps were thresholded at $p < 0.05$, FWE-corrected.

Mixed effects models were used to model the evolution over time (from baseline) of mean DT MRI metrics within each selected WM ROI. For each DT MRI measure, both a linear (LME) and a nonlinear mixed-effects (NLME) model were estimated to investigate which could better fit the longitudinal trend. Final models were obtained with a backward procedure of variable selection on the fixed-effects covariates. The best model (among the two final ones) was chosen as the one with the lowest Akaike Information Criteria (AIC). Outliers which have been observed for both starting models were excluded from the analysis of that MRI parameter. Due to the shape of the trajectories, the NLME model was defined as either a decreasing or an increasing exponential function with horizontal left asymptote. In case of the decreasing trend (used for FA), the equation of the model (Model 1) was:

$$MRImeasure = Asym(1 - \exp(time - xdec10 + \ln(0.1))),$$

while in case of an increasing function (used for diffusivity measures) this was (Model 2):

$$MRImeasure = Asym(1 + \exp(time - xinc10 + \ln(0.1))),$$

where *Asym* was the horizontal left asymptote (representing the "starting value"), while *xdec*10 or *xinc*10 describe the time to a 10% decrease or increase for MRI measure, respectively, with respect to the asymptote. In both LME and NLME models, we assessed the effect of fixed-effects covariates (sex, age at onset, ALSFRS-r score at baseline and the value of the selected MRI parameter at baseline) on the change of each MRI parameter over time (i.e., the slope in the LME model or the 10% increase/decrease relative to the horizontal left asymptote in the NLME model) was influenced by sex, age at onset, ALSFRS-r score at baseline and the value of the selected MRI parameter at baseline. Moreover, we evaluated whether the starting value of the MRI measure (i.e., the intercept in the LME model and the asymptote in the NLME model) was affected by sex, age at baseline and ALSFRS-r score at baseline. The random effects were set on the parameter representing the starting value (namely, the intercept for the LME model and the intercept of the asymptote in the NLME model), in order to account for the heterogeneity of values of the MRI measure among patients at baseline. For all DT MRI measures the best model resulted to be the appropriate NLME model (see Appendix). This analysis was performed using the nlme R package with R version 3.5.0 (http://www.R-project.org/).

2.5.3. Clinico-anatomical correlations

In ALS patients, voxel-wise regression models were run to test the association between the rate of decline of ALSFRS-r and the slopes of DT MRI measures within the WM skeleton obtained from TBSS, using the "randomize" voxel-wise statistical tool in FSL (permutations = 5000). Statistical maps were thresholded at $p < 0.05$, FWE-corrected.

In addition, a nonlinear mixed-effects model with a logistic shape was used to test the relationship between sex, age at onset and the value of FA of each selected WM ROIs at baseline and the subsequent rate of ALSFRS-r decline, using the following equation:

$$ALSFRS - r\ score = \frac{Asym}{1 + \exp\left[\frac{xmid - time}{scale}\right]}$$

where *Asym* represented the left horizontal asymptote (i.e., the "starting value" of ALSFRS-r), while the right horizontal asymptote (i.e., the "final value") was set to 0, as the value of ALSFRS-r at the eventual time-point corresponding to the occurrence of tracheostomy/

death was imputed as equivalent to this score; *xmid* represented the follow-up time (*time*) at which the ALSFRS-r score was midway between the asymptotes (thus indicating of a faster/slower progression rate); whereas *scale* was a scaling factor, which was set equal for all patients. We assessed whether the progression of the ALSFRS-r score over time (i.e., *xmid*) depended on the following fixed-effects covariates: sex, age at onset and the value of FA of the selected WM ROIs at baseline. The random effects were set on the intercept of *xmid* in order to account for the heterogeneity among patients in the rate of disease progression. We also evaluated whether the starting value of the ALSFRS-r score (*Asym*) depended on the following fixed-effects covariates: sex, age at baseline and disease duration at baseline. The final model was obtained by using a backward selection procedure on the fixed-effects covariates. The observations which were outliers for the starting model were eliminated from the analysis. This analysis was performed using the nlme R package with R version 3.5.0 (http://www.R-project.org/).

2.6. Sample size calculation

A minimum sample size was calculated for assessing a change at 6 months of either FA values of the bulbo-spinal CST (for this analysis, considered as representative for the whole CST) or ALSFRS-r, using data from the literature for identifying the target differences (Bede and Hardiman, 2018; Cardenas-Blanco et al., 2016; Kassubek et al., 2018). A sample of 28 patients was calculated as sufficient for showing a mean difference of bulbo-spinal CST FA values between 6 months and the baseline of −0.004 with standard deviation (SD) of 0.007, by considering 80% power and 5% significant level. By assuming a (conservative) moderate correlation between ALSFRS-r values at baseline and at 6 months (i.e., between 0.5 and 0.7), a sample size between 15 and 23 was computed as sufficient for showing a decrease from 40 (with SD = 5) to 36 (with SD = 7), by considering 80% power and 5% significant level. For comparison, Fig. 1 reports the numbers of available timepoints of the present cohort.

3. Results

3.1. Clinical evaluation

Table 1 reports the main demographic, clinical and cognitive data of participants. Forty-one ALS patients (i.e., 82%) met the survival endpoint (i.e., death or tracheostomy) at the time of censoring. All patients with a diagnosis of possible ALS at baseline had converted to a higher level of diagnostic certainty by the end of the available follow-up.

3.2. Baseline MRI findings

Cortical thickness. In ALS patients, no significant cortical thinning was detected relative to healthy controls at baseline.

WM voxel-wise analysis. On the baseline TBSS analysis, ALS patients showed extensively decreased FA relative to controls along the CST, bilaterally, and in the CC-body (Fig. 2-a, $p < 0.05$ FWE-corrected). Decreased FA was also found in the superior longitudinal fasciculi and frontal subcortical WM, bilaterally. No significant alterations of MD, axD, or radD were found.

WM ROI analysis. At baseline, the DT-derived measures showing significant alterations at a regional level in ALS patients were the mean FA values of CC-body ($p = 0.008$) and all CST ROIs ($p = 0.008$ for bulbo-pontine, $p < 0.001$ for other subregions), as well as MD values of the upper CST (superior corona radiata, $p = 0.008$; PLIC, $p = 0.048$) (Table 2). Other diffusivity metrics did not differ significantly from healthy controls.

3.3. Longitudinal MRI changes

Cortical thickness. In ALS patients, no significant cortical thinning over the 1-year MRI follow-up was detected.

WM voxel-wise analysis. A significant evolution of microstructural WM damage was found, in terms of decreased FA and increased MD, axD and radD (Fig. 2-b, $p < 0.05$ FWE-corrected). MD and radD, which did not show significant alterations at baseline, increased over time not only along the CSTs and the CC-body, but also in the genu of the CC, bilateral superior longitudinal fasciculi and anterior corona radiata, and left inferior longitudinal fasciculus. FA decreased significantly in the same areas, except for the CSTs. The longitudinal increase of axD involved only a restricted area including the genu of the CC, the PLIC and the superior-anterior corona radiata of the right hemisphere.

WM ROI analysis. The evolution over time of mean FA, MD and radD values within each selected ROI (i.e., body-CC and 4 CST subregions) was modelled using both a linear and a nonlinear mixed-effects (NLME) model. For all DT MRI measures, the best model resulted to be the nonlinear one. Fig. 3, Supplementary Fig. 1 and Supplementary Fig. 2 show the progression of such values for each subject over time, together with the corresponding estimated model. Considering the modest size and localization of axD increase in the voxel-wise analysis, we did not model the longitudinal evolution of this measure within the ROIs. The estimated models are reported in the Appendix. Damage to the CC-body and CST subregions consistently showed faster progression in ALS patients with higher ALSFRS-r at baseline (FA of the CC-body, MD of the bulbo-pontine CST, FA/MD/radD of the cerebral peduncle and PLIC). Greater WM damage at baseline was also associated with faster subsequent decline of FA/MD/radD of the CC-body, and FA of the PLIC, although an opposite association was found for radD of the PLIC. Female sex was mostly associated with faster WM deterioration (MD of the CC-body, FA/radD of the bulbo-pontine CST, FA of the PLIC, FA/MD/radD of the superior corona radiata), although male patients showed faster progression of radD of the PLIC. Younger age at onset was associated with faster decline of FA/MD/radD of the CC-body, FA of the cerebral peduncle, and MD/radD of the PLIC, whereas an opposite association was shown for FA of the bulbo-pontine CST and MD of the superior corona radiata.

3.4. Relationship between structural brain changes and clinical progression in ALS patients

Voxel-wise regression models showed a significant association between the slopes of ALSFRS-r progression and FA decrease within WM fibers of the CC-body (Fig. 2-c).

The progression of the ALSFRS-r score over time, as assessed using the NLME model, was found to occur faster in ALS patients with lower baseline FA of the cerebral peduncle ($p = 0.047$), indicating this DT MRI measure as a predictor of more rapid subsequent functional decline. The starting value of ALSFRS-r showed, as expected, an inverse association with disease duration ($p = 0.049$; Fig. 4, Table 3). Other demographic (i.e., age at onset, sex) and MRI measures were not significantly related with ALSFRS-r progression over time.

4. Discussion

In this longitudinal study, a whole-brain voxel-wise approach with no *a priori* assumptions was adopted to identify which MRI measures were the most sensitive to early and progressive brain damage in ALS patients enrolled within one year from clinical diagnosis, who showed consequently mild disease severity at baseline (mean ALSFRS-

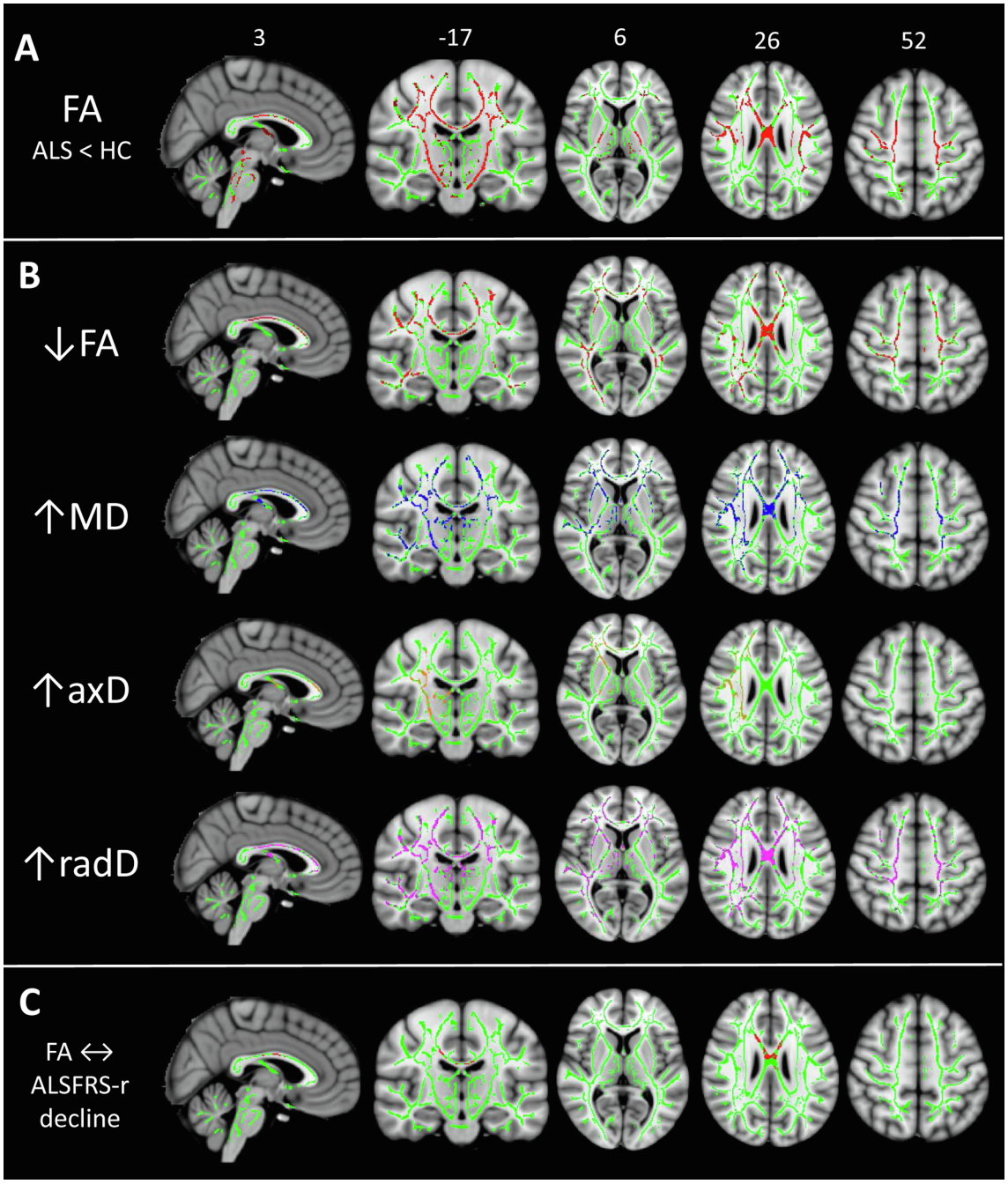

Fig. 2. Results of white matter (WM) voxel-wise analysis: A) cross-sectional results of TBSS analysis comparing ALS patients with healthy controls at baseline; B) regions of significant decrease/increase of DT MRI metrics over time, as measured in terms of slopes of FA (red), MD (blue), axD (orange), or radD (violet) change; and C) regions of significant correlation between ALSFRS-r and FA decline over follow-up time. All results are superimposed on the WM skeleton of TBSS (light green) and on the Montreal Neurological Institute (MNI) template, thresholded at $p < 0.05$ FWE-corrected, and adjusted for age and sex. Results displayed in B) and C) are also adjusted for baseline ALSFRS-r values. *Abbreviations: ALS = amyotrophic lateral sclerosis; ALSFRS-r = ALS Functional Rating Scale, revised version, axD = axial diffusivity; CST = corticospinal tract; DT = diffusion tensor; MD = mean diffusivity; radD = radial diffusivity; TBSS = Tract-based Spatial Statistics; WM = white matter.* (For interpretation of the references to colour in this figure legend, the reader is referred to the web version of this article.)

r = 41.5 ± 5.1). We found consistent alterations of MRI measures of WM microstructural integrity that were mostly restricted to the CC-body and CST at baseline and later progressed to involve widespread anterior frontal, temporal and parietal tracts over a one-year follow-up time in ALS patients. DT MRI metrics showed progressive worsening over time that was influenced by several demographic, clinical and MRI features. FA decrease in the CC-body was found to correlate with the progression of ALSFRS-r, whereas baseline FA values of the cerebral peduncle predicted a more rapid subsequent clinical course. By contrast, no significant cortical thinning was detected either at baseline or over time.

Results from previous longitudinal MRI studies in ALS are conflicting as regards the relative impact of pathology progression over cortical GM and WM disruption. In fact, some have suggested a key role of GM atrophy over time (Bede and Hardiman, 2018; Kwan et al., 2012; Menke et al., 2018), whereas others found no significant longitudinal cortical changes (de Albuquerque et al., 2017; Schuster et al., 2014; Verstraete et al., 2014). Progression of WM damage demonstrated by

Table 2
Mean DT MRI measures of the selected WM regions of interest (ROIs) in ALS patients and healthy controls (HC).

Variable	HC	ALS patients	*p*
FA CC-body	0.684 ± 0.04	0.664 ± 0.037	**0.008**
FA Bulbo-pontine CST	0.618 ± 0.035	0.599 ± 0.033	**0.008**
FA Cerebral peduncle	0.712 ± 0.023	0.69 ± 0.025	< **0.001**
FA Posterior internal capsule	0.69 ± 0.024	0.671 ± 0.025	< **0.001**
FA Superior corona radiata	0.49 ± 0.028	0.471 ± 0.022	< **0.001**
MD CC-body	0.84 ± 0.059	0.847 ± 0.057	0.600
MD Bulbo-pontine CST	0.685 ± 0.042	0.695 ± 0.03	0.212
MD Cerebral peduncle	0.718 ± 0.031	0.722 ± 0.032	0.639
MD Posterior internal capsule	0.704 ± 0.022	0.714 ± 0.024	**0.048**
MD Superior corona radiata	0.719 ± 0.028	0.736 ± 0.030	**0.008**
axD CC-body	1.641 ± 0.067	1.618 ± 0.067	0.06
axD Bulbo-pontine CST	1.21 ± 0.067	1.204 ± 0.067	0.553
axD Cerebral peduncle	1.425 ± 0.071	1.406 ± 0.055	0.082
axD Posterior internal capsule	1.374 ± 0.055	1.366 ± 0.044	0.293
axD Superior corona radiata	1.143 ± 0.047	1.151 ± 0.048	0.542
radD CC-body	0.449 ± 0.083	0.461 ± 0.063	0.428
radD Bulbo-pontine CST	0.432 ± 0.083	0.44 ± 0.03	0.610
radD Cerebral peduncle	0.367 ± 0.058	0.38 ± 0.031	0.206
radD Posterior internal capsule	0.377 ± 0.059	0.389 ± 0.027	0.255
radD Superior corona radiata	0.518 ± 0.08	0.529 ± 0.027	0.484

Values are reported as mean ± standard deviation. Differences between ALS patients and healthy controls were assessed using a Multivariate Analysis of Covariance (MANCOVA) test, adjusting for sex and age and applying Bonferroni correction. *Abbreviations: ALS = amyotrophic lateral sclerosis; axD = axial diffusivity; CC = corpus callosum; CST = corticospinal tract; FA = fractional anisotropy; MD = mean diffusivity; HC = healthy controls; radD = radial diffusivity.* Bold is for significant values

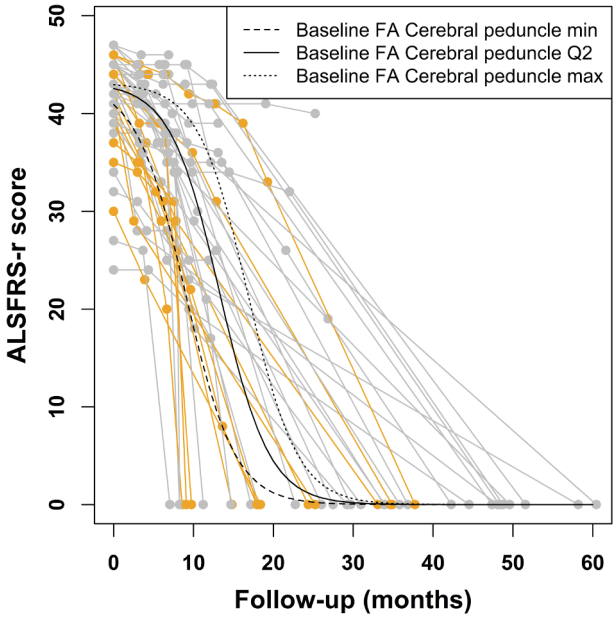

Fig. 4. Nonlinear mixed-effects model describing the ALSFRS-r evolution over follow-up time from baseline. Individual scores are represented in grey for male patients and in orange for female patients, whereas the curves represent the estimated model by varying the baseline FA of the cerebral peduncle. *Abbreviations: ALSFRS-r = ALS Functional Rating Scale, revised version; CST = corticospinal tract; FA = fractional anisotropy; Q2 = median.* (For interpretation of the references to colour in this figure legend, the reader is referred to the web version of this article.)

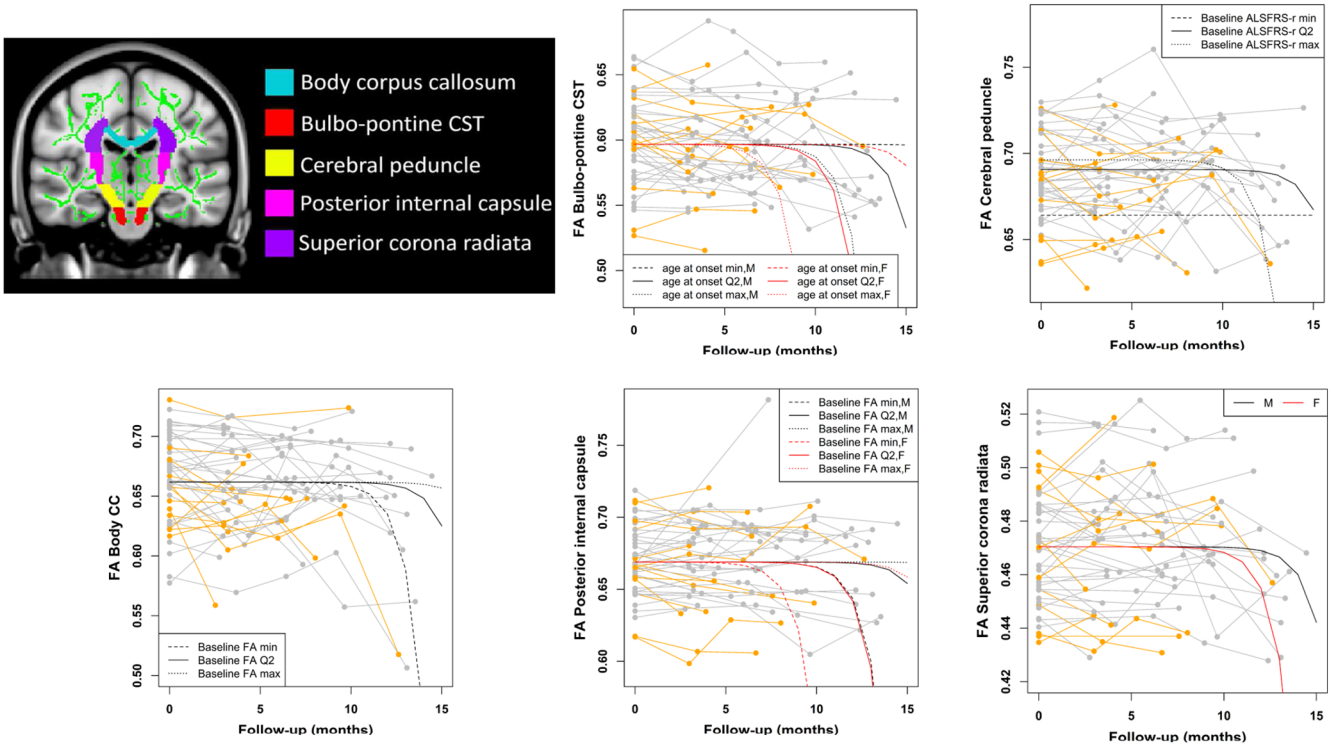

Fig. 3. Regions of interest (ROIs) selected from the Johns Hopkins University (JHU) white-matter tractography atlas, superimposed on the Montreal Neurological Institute (MNI) template (in the top left corner), and plots showing the longitudinal evolution of FA for each selected ROI over follow-up time from baseline, together with the corresponding nonlinear mixed-effects model. Individual FA values are represented in grey for male patients and in orange for female patients, whereas the curves represent the estimated models by varying the values of some covariates in the model. When not specified, the covariates were set equal to the median value. *Abbreviations: CC = corpus callosum; CST = corticospinal tract; DT = diffusion tensor; FA = fractional anisotropy; ROI = region of interest; WM = white matter.* (For interpretation of the references to colour in this figure legend, the reader is referred to the web version of this article.)

Table 3
Nonlinear mixed-effects model analyzing the longitudinal evolution of ALSFRS-r from baseline in ALS patients.

Parameter	Coefficient	SE	*p* value
xmid (i.e., *50% decrease of ALSFRS-r)*			
Intercept	−43.833	28.454	0.013
Baseline FA of Cerebral peduncle	83.085	41.435	0.047
Asym (i.e., *starting value of ALSFRS-r)*			
Intercept	44.200	0.803	< 0.001
Disease duration at baseline	−0.078	0.039	0.049
Scale	3.098	0.224	< 0.001

Positive values of the estimated coefficients, in the submodel of the parameter *xmid,* indicate that 50% decrease of ALSFRS-r is reached later as the corresponding variable increases; whereas, in the submodel of the parameter *Asym*, positive values indicate that the starting value of ALSFRS-r is higher as the corresponding variable increases. *Abbreviations: ALS = amyotrophic lateral sclerosis; ALSFRS-r = ALS Functional Rating Scale, revised version; CST = corticospinal tract; FA = fractional anisotropy; SE = standard error.*

DT MRI has been reported more consistently (Bede and Hardiman, 2018; de Albuquerque et al., 2017; Kassubek et al., 2018; Keil et al., 2012; Menke et al., 2018; Steinbach et al., 2015), although a minority of studies could not detect such longitudinal evolution (Agosta et al., 2009; Kwan et al., 2012), and some variability regarding the entity and the pattern of such progression likely derive from the heterogeneous disease course and great variability across studies in sample sizes, follow-up intervals and functional impairment at baseline.

In our study, no cross-sectional or longitudinal cortical thinning was detected at a statistical threshold corrected for multiple comparisons, after adjusting for age and sex. The lack of GM alterations in ALS patients even at baseline contrasts with previous results from our (Spinelli et al., 2016) and other research groups (Kwan et al., 2012; Verstraete et al., 2010), but is likely due to the shorter disease duration and milder disability of the present sample, as well as to the use of different statistical approaches. By contrast, the identification of the known signature of FA decrease relative to healthy controls at baseline, encompassing the CST in its entirety and the motor callosal fibers (i.e., the CC-body), was expected and consistent with previous reports from several research groups (Agosta et al., 2014; Bede and Hardiman, 2018; Kassubek et al., 2018; Schuster et al., 2016) and a recent large multicenter study pooling DT MRI data of ALS patients from eight sites (Muller et al., 2016). The cross-sectional, ROI-based analysis confirmed such difference when averaged values within each motor tract ROI (i.e., four CST subregions and CC-body) were considered. In particular, FA was the earliest DT-derived measure to be altered, whereas diffusivity metrics were relatively spared at baseline, with the exception of MD of the superior corona radiata and PLIC. This is in keeping with previous studies showing most widespread baseline alterations of FA in ALS cohorts (Agosta et al., 2014; Bede and Hardiman, 2018; de Albuquerque et al., 2017), possibly consistent with early axonal degeneration. On the other hand, a longitudinal analysis that considered all available timepoints within a one-year follow-up demonstrated progression of FA, MD and radD alterations in widespread WM regions, involving not only motor tracts, but also extra-motor fronto-temporo-parietal WM. This is in line with the pattern described by previous reports (Bede and Hardiman, 2018; Menke et al., 2018) and mirrors the pathological staging described by Brettschneider et al. (Brettschneider et al., 2013), although a strict correspondence is difficult to draw, as this staging is based on TDP-43 depositions in the cortical GM. When our longitudinal analysis focused on the ROIs of the motor tracts, FA decrease and MD/radD increase in ALS patients showed a non-linear evolution over time with a complex dependence on demographic, clinical and MRI features, as further discussed below. Taken together, our results suggest that advanced structural MRI techniques assessing WM integrity might have greater sensitivity to early damage and subsequent evolution of ALS pathology, compared with those evaluating GM.

The longitudinal analysis of WM alterations within the selected ROIs has provided some intriguing suggestions regarding the pattern and timing of DT MRI alterations in ALS patients. Particularly, the association of a more rapid WM disruption within these regions with higher baseline ALSFRS-r values and, for the CC-body, greater baseline MRI alterations suggests, on the one hand, that WM microstructural rearrangements occur early in ALS disease course, even before the development of a severe functional impairment; on the other hand, that once WM degeneration of the callosal fibers has started, this does not tend towards reaching a plateau, but rather to a greater rate of deterioration, at least in the early phases covered by the 1-year timeframe of the present MRI study. The relationship of WM longitudinal damage with other demographic features (i.e., sex and age) is more difficult to interpret, as our results showed diverging consequences of the same factors across different WM subregions (although female sex was most consistently associated with faster WM disruption). The complex influence of these factors over DT MRI metrics has been explored only recently in different contexts (i.e., healthy aging and pathological conditions, including ALS) (Bede et al., 2014; O'Dwyer et al., 2012; Rathee et al., 2016). In the present study, given the absence of longitudinal data of healthy controls, it is impossible to discriminate between the "normal" influence of demographic features over WM integrity and their interaction with disease status, although demographic factors have been indicated as fundamental prognostic factors (Calvo et al., 2017; Chio et al., 2020) and previous neuroimaging evidence suggests significant sexual dimorphism in the evolution of ALS pathology (Bede et al., 2014).

This study has also identified significant associations between measures of WM damage of the motor tracts and functional decline in ALS patients. FA decrease of the CC-body correlated with the decline of ALSFRS-r (Fig. 2-c), suggesting that functional decline in ALS might at least partially derive from an interhemispheric disconnection between contralateral motor networks. This is in line with previous studies showing a significant association between WM motor tract degeneration and worsening disability (Kassubek et al., 2018; Keil et al., 2012; Menke et al., 2018), and supports these measures as possible additional quantitative outcomes – more specifically related to CNS damage compared with ALSFRS-r – when following disease evolution. Moreover, we demonstrated that decreased FA of the cerebral peduncle is an independent predictor of a faster subsequent ALSFRS-r decline (Fig. 4, Table 3). The cerebral peduncle has already been indicated as a key region to discriminate ALS patients from controls based on DT MRI, even more than other CST subregions (Schuster et al., 2016). Moreover, the process of tract reconstruction in the cerebral peduncle might be less affected by the presence of crossing fibers, when compared to other CST subregions (Mandelli et al., 2014), possibly making this measure more closely related to the underlying WM pathology. Therefore, it is not surprising that greater damage to this region might also have a prognostic, as well as diagnostic role in ALS. This finding integrates previous studies specifically assessing DT MRI measures of the CST for a prediction of survival (Agosta et al., 2019; Schuster et al., 2017; van der Burgh et al., 2017), and strongly suggests that a multimodal approach including such measures would provide an optimal method for an accurate prognostic stratification of ALS patients.

Compared with previous studies adopting a similar multiparametric MRI approach (Bede and Hardiman, 2018; de Albuquerque et al., 2017; Menke et al., 2018), we were able to enroll a well-sized sample of patients who underwent at least 2 MRI scans over the follow up, strengthening our claim that the lack of significant GM alterations is not due to an insufficient sample. A limitation of this longitudinal study is the relatively high attrition rate, as only 18/50 patients could undergo the last, 12-month MRI scan. However, this was expected given the aggressive course of ALS; moreover, the specific statistical design that we used was meant to take into account missing values and differences in follow-up time. Another limitation was the unavailability of longitudinal data of healthy controls, although this did not affect the main

focus of our study, which was on identifying the structural MRI alterations that were most sensitive to ALS clinical progression and could contribute to predict a faster functional deterioration.

Despite these limitations, our data allow to conclude that DT MRI metrics are sensitive to brain damage in the first stages of ALS and can provide useful information to monitor disease progression and aid in the prognostic stratification of patients. Larger samples will be needed to further explore these suggestions in specific subpopulations (e.g., according to site of onset, different cognitive status, etc.).

CRediT authorship contribution statement

Edoardo G. Spinelli: Conceptualization, Data curation, Formal analysis, Investigation, Methodology, Writing - original draft, Writing - review & editing. **Nilo Riva:** Investigation, Methodology, Writing - review & editing. **Paola M.V. Rancoita:** Formal analysis, Methodology, Software, Writing - review & editing. **Paride Schito:** Investigation, Writing - review & editing. **Alberto Doretti:** Investigation, Writing - review & editing. **Barbara Poletti:** Investigation, Writing - review & editing. **Clelia Di Serio:** Methodology, Writing - review & editing. **Vincenzo Silani:** Investigation, Funding acquisition, Resources, Writing - review & editing. **Massimo Filippi:** Conceptualization, Funding acquisition, Resources, Supervision, Writing - review & editing. **Federica Agosta:** Conceptualization, Methodology, Project administration, Resources, Supervision, Writing - review & editing.

Declaration of Competing Interest

The authors declare that they have no known competing financial interests or personal relationships that could have appeared to influence the work reported in this paper.

Acknowledgments

The authors thank the patients and their families for the time and effort they dedicated to the research.

Funding

This study was partially supported by the Italian Ministry of Health (grants #RF-2010-2313220 and #RF-2011-02351193).

Disclosures

E.G. Spinelli, N. Riva, PMV Rancoita, A. Doretti, B. Poletti, and C. Di Serio report no disclosures.

V. Silani is in the Editorial Board of Amyotroph Lateral Sclerosis, European Neurology, American Journal of Neurodegenerative Diseases, Frontiers in Neurology; received compensation for consulting services and/or speaking activities from AveXis, Cytokinetics, and Italfarmaco; and receives or has received research supports from the Italian Ministry of Health, AriSLA (Fondazione Italiana di Ricerca per la SLA), and E-Rare Joint Transnational Call.

M. Filippi is Editor-in-Chief of the Journal of Neurology; received compensation for consulting services and/or speaking activities from Bayer, Biogen Idec, Merck-Serono, Novartis, Roche, Sanofi Genzyme, Takeda, and Teva Pharmaceutical Industries; and receives research support from Biogen Idec, Merck-Serono, Novartis, Roche, Teva Pharmaceutical Industries, Italian Ministry of Health, Fondazione Italiana Sclerosi Multipla, and ARiSLA (Fondazione Italiana di Ricerca per la SLA).

F. Agosta is Section Editor of NeuroImage: Clinical; has received speaker honoraria from Novartis, Biogen Idec and Philips; and receives or has received research supports from the Italian Ministry of Health, AriSLA (Fondazione Italiana di Ricerca per la SLA), and the European Research Council.

Supported by: Italian Ministry of Health (RF-2010–2313220; RF-2011–02351193).

Appendix A. Supplementary data

Supplementary data to this article can be found online at https://doi.org/10.1016/j.nicl.2020.102315.

References

Agosta, F., Galantucci, S., Canu, E., Cappa, S.F., Magnani, G., Franceschi, M., Falini, A., Comi, G., Filippi, M., 2013. Disruption of structural connectivity along the dorsal and ventral language pathways in patients with nonfluent and semantic variant primary progressive aphasia: a DT MRI study and a literature review. Brain Lang 127, 157–166.

Agosta, F., Galantucci, S., Riva, N., Chio, A., Messina, S., Iannaccone, S., Calvo, A., Silani, V., Copetti, M., Falini, A., Comi, G., Filippi, M., 2014. Intrahemispheric and inter-hemispheric structural network abnormalities in PLS and ALS. Hum Brain Mapp 35, 1710–1722.

Agosta, F., Rocca, M.A., Valsasina, P., Sala, S., Caputo, D., Perini, M., Salvi, F., Prelle, A., Filippi, M., 2009. A longitudinal diffusion tensor MRI study of the cervical cord and brain in amyotrophic lateral sclerosis patients. J Neurol Neurosurg Psychiatry 80, 53–55.

Agosta, F., Spinelli, E.G., Filippi, M., 2018. Neuroimaging in amyotrophic lateral sclerosis: current and emerging uses. Expert Rev Neurother 18, 395–406.

Agosta, F., Spinelli, E.G., Riva, N., Fontana, A., Basaia, S., Canu, E., Castelnovo, V., Falzone, Y., Carrera, P., Comi, G., Filippi, M., 2019. Survival prediction models in motor neuron disease. Eur J Neurol 26, 1143–1152.

Bede, P., Elamin, M., Byrne, S., Hardiman, O., 2014. Sexual dimorphism in ALS: exploring gender-specific neuroimaging signatures. Amyotroph Lateral Scler Frontotemporal Degener 15, 235–243.

Bede, P., Hardiman, O., 2018. Longitudinal structural changes in ALS: a three time-point imaging study of white and gray matter degeneration. Amyotroph Lateral Scler Frontotemporal Degener 19, 232–241.

Bernal-Rusiel, J.L., Reuter, M., Greve, D.N., Fischl, B., Sabuncu, M.R., Neuroimaging, Alzheimer's Disease, I, 2013. Spatiotemporal linear mixed effects modeling for the mass-univariate analysis of longitudinal neuroimage data. Neuroimage 81, 358–370.

Brettschneider, J., Del Tredici, K., Toledo, J.B., Robinson, J.L., Irwin, D.J., Grossman, M., Suh, E., Van Deerlin, V.M., Wood, E.M., Baek, Y., Kwong, L., Lee, E.B., Elman, L., McCluskey, L., Fang, L., Feldengut, S., Ludolph, A.C., Lee, V.M., Braak, H., Trojanowski, J.Q., 2013. Stages of pTDP-43 pathology in amyotrophic lateral sclerosis. Ann Neurol 74, 20–38.

Brooks, B.R., Miller, R.G., Swash, M., Munsat, T.L., World Federation of Neurology Research Group on Motor Neuron, D., 2000. El Escorial revisited: revised criteria for the diagnosis of amyotrophic lateral sclerosis. Amyotroph Lateral Scler Other Motor Neuron Disord 1, 293-299.

Calvo, A., Moglia, C., Lunetta, C., Marinou, K., Ticozzi, N., Ferrante, G.D., Scialo, C., Soraru, G., Trojsi, F., Conte, A., Falzone, Y.M., Tortelli, R., Russo, M., Chio, A., Sansone, V.A., Mora, G., Silani, V., Volanti, P., Caponnetto, C., Querin, G., Monsurro, M.R., Sabatelli, M., Riva, N., Logroscino, G., Messina, S., Fini, N., Mandrioli, J., 2017. Factors predicting survival in ALS: a multicenter Italian study. J Neurol 264, 54–63.

Cardenas-Blanco, A., Machts, J., Acosta-Cabronero, J., Kaufmann, J., Abdulla, S., Kollewe, K., Petri, S., Schreiber, S., Heinze, H.J., Dengler, R., Vielhaber, S., Nestor, P.J., 2016. Structural and diffusion imaging versus clinical assessment to monitor amyotrophic lateral sclerosis. Neuroimage Clin 11, 408–414.

Cedarbaum, J.M., Stambler, N., Malta, E., Fuller, C., Hilt, D., Thurmond, B., Nakanishi, A., 1999. The ALSFRS-R: a revised ALS functional rating scale that incorporates assessments of respiratory function. BDNF ALS Study Group (Phase III). J Neurol Sci 169, 13–21.

Chio, A., Moglia, C., Canosa, A., Manera, U., D'Ovidio, F., Vasta, R., Grassano, M., Brunetti, M., Barberis, M., Corrado, L., D'Alfonso, S., Iazzolino, B., Peotta, L., Sarnelli, M.F., Solara, V., Zucchetti, J.P., De Marchi, F., Mazzini, L., Mora, G., Calvo, A., 2020. ALS phenotype is influenced by age, sex, and genetics: A population-based study. Neurology 94, e802–e810.

Dale, A.M., Fischl, B., Sereno, M.I., 1999. Cortical surface-based analysis. I. Segmentation and surface reconstruction. Neuroimage 9, 179–194.

de Albuquerque, M., Branco, L.M., Rezende, T.J., de Andrade, H.M., Nucci, A., Franca Jr., M.C., 2017. Longitudinal evaluation of cerebral and spinal cord damage in Amyotrophic Lateral Sclerosis. Neuroimage Clin 14, 269–276.

Fischl, B., Dale, A.M., 2000. Measuring the thickness of the human cerebral cortex from magnetic resonance images. Proc Natl Acad Sci U S A 97, 11050–11055.

Folstein, M.F., Folstein, S.E., McHugh, P.R., 1975. "Mini-mental state". A practical method for grading the cognitive state of patients for the clinician. J Psychiatr Res 12, 189–198.

Horsfield, M.A., 1999. Mapping eddy current induced fields for the correction of diffusion-weighted echo planar images. Magn Reson Imaging 17, 1335–1345.

Hua, K., Zhang, J., Wakana, S., Jiang, H., Li, X., Reich, D.S., Calabresi, P.A., Pekar, J.J., van Zijl, P.C., Mori, S., 2008. Tract probability maps in stereotaxic spaces: analyses of white matter anatomy and tract-specific quantification. Neuroimage 39, 336–347.

Kassubek, J., Muller, H.P., Del Tredici, K., Lule, D., Gorges, M., Braak, H., Ludolph, A.C., 2018. Imaging the pathoanatomy of amyotrophic lateral sclerosis in vivo: targeting a propagation-based biological marker. J Neurol Neurosurg Psychiatry 89, 374–381.

Keil, C., Prell, T., Peschel, T., Hartung, V., Dengler, R., Grosskreutz, J., 2012. Longitudinal diffusion tensor imaging in amyotrophic lateral sclerosis. BMC Neurosci 13, 141.

Kiernan, M.C., Vucic, S., Cheah, B.C., Turner, M.R., Eisen, A., Hardiman, O., Burrell, J.R., Zoing, M.C., 2011. Amyotrophic lateral sclerosis. Lancet 377, 942–955.

Kwan, J.Y., Meoded, A., Danielian, L.E., Wu, T., Floeter, M.K., 2012. Structural imaging differences and longitudinal changes in primary lateral sclerosis and amyotrophic lateral sclerosis. Neuroimage Clin 2, 151–160.

Mandelli, M.L., Berger, M.S., Bucci, M., Berman, J.I., Amirbekian, B., Henry, R.G., 2014. Quantifying accuracy and precision of diffusion MR tractography of the corticospinal tract in brain tumors. J Neurosurg 121, 349–358.

Menke, R.A., Agosta, F., Grosskreutz, J., Filippi, M., Turner, M.R., 2017. Neuroimaging Endpoints in Amyotrophic Lateral Sclerosis. Neurotherapeutics 14, 11–23.

Menke, R.A.L., Proudfoot, M., Talbot, K., Turner, M.R., 2018. The two-year progression of structural and functional cerebral MRI in amyotrophic lateral sclerosis. Neuroimage Clin 17, 953–961.

Muller, H.P., Turner, M.R., Grosskreutz, J., Abrahams, S., Bede, P., Govind, V., Prudlo, J., Ludolph, A.C., Filippi, M., Kassubek, J., Neuroimaging Society in, A.L.S.D.T.I.S.G., 2016. A large-scale multicentre cerebral diffusion tensor imaging study in amyotrophic lateral sclerosis. J Neurol Neurosurg Psychiatry 87, 570-579.

Novelli, G., Papagno, C., Capitani, E., Laiacona, M., Vallar, G., Cappa, S., 1986. Tre test clinici di ricerca e produzione lessicale. Taratura su soggetti normali. Archivio di Psicologia, Neurologia e Psichiatria. oct-dec; vol 47 (4) : 477-506.

O'Dwyer, L., Lamberton, F., Bokde, A.L., Ewers, M., Faluyi, Y.O., Tanner, C., Mazoyer, B., O'Neill, D., Bartley, M., Collins, R., Coughlan, T., Prvulovic, D., Hampel, H., 2012. Sexual dimorphism in healthy aging and mild cognitive impairment: a DTI study. PLoS One 7, e37021.

Rascovsky, K., Hodges, J.R., Knopman, D., Mendez, M.F., Kramer, J.H., Neuhaus, J., van Swieten, J.C., Seelaar, H., Dopper, E.G., Onyike, C.U., Hillis, A.E., Josephs, K.A., Boeve, B.F., Kertesz, A., Seeley, W.W., Rankin, K.P., Johnson, J.K., Gorno-Tempini, M.L., Rosen, H., Prioleau-Latham, C.E., Lee, A., Kipps, C.M., Lillo, P., Piguet, O., Rohrer, J.D., Rossor, M.N., Warren, J.D., Fox, N.C., Galasko, D., Salmon, D.P., Black, S.E., Mesulam, M., Weintraub, S., Dickerson, B.C., Diehl-Schmid, J., Pasquier, F., Deramecourt, V., Lebert, F., Pijnenburg, Y., Chow, T.W., Manes, F., Grafman, J., Cappa, S.F., Freedman, M., Grossman, M., Miller, B.L., 2011. Sensitivity of revised diagnostic criteria for the behavioural variant of frontotemporal dementia. Brain 134, 2456–2477.

Rathee, R., Rallabandi, V.P., Roy, P.K., 2016. Age-Related Differences in White Matter Integrity in Healthy Human Brain: Evidence from Structural MRI and Diffusion Tensor Imaging. Magn Reson Insights 9, 9–20.

Reuter, M., Schmansky, N.J., Rosas, H.D., Fischl, B., 2012. Within-subject template estimation for unbiased longitudinal image analysis. Neuroimage 61, 1402–1418.

Schuster, C., Elamin, M., Hardiman, O., Bede, P., 2016. The segmental diffusivity profile of amyotrophic lateral sclerosis associated white matter degeneration. Eur J Neurol 23, 1361–1371.

Schuster, C., Hardiman, O., Bede, P., 2017. Survival prediction in Amyotrophic lateral sclerosis based on MRI measures and clinical characteristics. BMC Neurol 17, 73.

Schuster, C., Kasper, E., Machts, J., Bittner, D., Kaufmann, J., Benecke, R., Teipel, S., Vielhaber, S., Prudlo, J., 2014. Longitudinal course of cortical thickness decline in amyotrophic lateral sclerosis. J Neurol 261, 1871–1880.

Spinelli, E.G., Agosta, F., Ferraro, P.M., Riva, N., Lunetta, C., Falzone, Y.M., Comi, G., Falini, A., Filippi, M., 2016. Brain MR Imaging in Patients with Lower Motor Neuron-Predominant Disease. Radiology 280, 545–556.

Steinbach, R., Loewe, K., Kaufmann, J., Machts, J., Kollewe, K., Petri, S., Dengler, R., Heinze, H.J., Vielhaber, S., Schoenfeld, M.A., Stoppel, C.M., 2015. Structural hallmarks of amyotrophic lateral sclerosis progression revealed by probabilistic fiber tractography. J Neurol 262, 2257–2270.

Turner, M.R., Cagnin, A., Turkheimer, F.E., Miller, C.C., Shaw, C.E., Brooks, D.J., Leigh, P.N., Banati, R.B., 2004. Evidence of widespread cerebral microglial activation in amyotrophic lateral sclerosis: an [11C](R)-PK11195 positron emission tomography study. Neurobiol Dis 15, 601–609.

van der Burgh, H.K., Schmidt, R., Westeneng, H.J., de Reus, M.A., van den Berg, L.H., van den Heuvel, M.P., 2017. Deep learning predictions of survival based on MRI in amyotrophic lateral sclerosis. Neuroimage Clin 13, 361–369.

van der Graaff, M.M., Sage, C.A., Caan, M.W., Akkerman, E.M., Lavini, C., Majoie, C.B., Nederveen, A.J., Zwinderman, A.H., Vos, F., Brugman, F., van den Berg, L.H., de Rijk, M.C., van Doorn, P.A., Van Hecke, W., Peeters, R.R., Robberecht, W., Sunaert, S., de Visser, M., 2011. Upper and extra-motoneuron involvement in early motoneuron disease: a diffusion tensor imaging study. Brain 134, 1211–1228.

Verstraete, E., van den Heuvel, M.P., Veldink, J.H., Blanken, N., Mandl, R.C., Hulshoff Pol, H.E., van den Berg, L.H., 2010. Motor network degeneration in amyotrophic lateral sclerosis: a structural and functional connectivity study. PLoS One 5, e13664.

Verstraete, E., Veldink, J.H., van den Berg, L.H., van den Heuvel, M.P., 2014. Structural brain network imaging shows expanding disconnection of the motor system in amyotrophic lateral sclerosis. Hum Brain Mapp 35, 1351–1361.